

Scale-dependent bias with higher order primordial non-Gaussianity: Use of the Integrated Perturbation Theory

Shuichiro Yokoyama^{1,*} and Takahiko Matsubara^{2,3,†}

¹*Institute for Cosmic Ray Research, The University of Tokyo, Kashiwa, Chiba, 277-8582, Japan*

²*Kobayashi-Maskawa Institute for the Origin of Particles and the Universe,
Nagoya University, Chikusa, Nagoya, 464-8602, Japan*

³*Department of Physics, Nagoya University, Chikusa, Nagoya, 464-8602, Japan*

We analytically derive a more accurate formula for the power spectrum of the biased objects with the primordial non-Gaussianity parameterized not only by the non-linearity parameter f_{NL} , but also by g_{NL} and τ_{NL} which characterize the trispectrum of the primordial curvature perturbations. We adopt the integrated perturbation theory which was constructed in Matsubara (2011) [1]. We discuss an inequality between f_{NL} and τ_{NL} in the context of the scale-dependent bias, by introducing a stochasticity parameter. We also mention higher order loop corrections into the scale-dependency of the bias parameter.

I. INTRODUCTION

Primordial non-Gaussianities have been widely well-studied as new probes of the mechanism of generating primordial curvature perturbation, e.g., inflationary physics. The observation of the cosmic microwave background (CMB) anisotropies is one of the best ways to hunt for the primordial non-Gaussianities through the measurement of the bi- and tri-spectra of the temperature anisotropies. For example, a current best limit for the primordial non-Gaussianity is obtained as $-10 < f_{\text{NL}} < 74$ at 95% confidence level (CL) [2] with f_{NL} being a local-type non-linearity parameter, which characterizes the bispectrum of the primordial curvature perturbations. The standard single field inflation model predicts that f_{NL} is the order of 10^{-2} and hence if we would detect that $f_{\text{NL}} > O(1)$ it implies that our universe has not experienced the standard inflationary stage with a single scalar field.

Thanks to the progress of the cosmological observations, recently, the large scale structure (LSS) of the universe will also bring us the fruitful information about the primordial fluctuations. While in the observation of LSS the understanding of the gravitational non-linear evolution of the density fluctuations is more important on smaller scales, the primordial non-Gaussianities affect the clustering of the biased objects on large scales. It has been found that the local-type primordial non-Gaussianity, f_{NL} , produces significant scale-dependence on the bias parameter, $\Delta b \propto 1/k^2$. The constraints on the primordial non-Gaussianities obtained from the observations of such scale-dependence of the bias are comparable to those from the CMB observations, e.g., $-31 < f_{\text{NL}} < 70$ at 95% CL in Ref. [3].

However, in order to make ready for the upcoming precise observational cosmology, on the theoretical side, more deeply understanding of the effect of the primordial non-Gaussianities should be necessary. There are a lot of literatures about the precise formula for the scale-dependent bias both analytically and numerically and also the analysis of the higher order effects. Recently, Matsubara (2012) [4] has shown an accurate formula of the scale-dependent bias with primordial non-Gaussianity parametrized by f_{NL} , by making use of the integrated Perturbation Theory (IPT) [1]. By adopting this formula, it is not necessary to use the high peak approximation and also the peak-background split picture, both of which have been considered as useful tools to derive the bias parameter in the case with the primordial non-Gaussianity.

Together with deriving the precise formula of the bias parameter for f_{NL} case (see, e.g., [5, 6]), it should be important to investigate the effects of the higher order primordial non-Gaussianities, that is, the trispectrum of the primordial curvature perturbations. The non-linearity parameters denoted by g_{NL} and τ_{NL} were introduced to characterize the amplitude of the primordial trispectrum. There are also lots of literatures which study these non-linearity parameters theoretically and observationally. One of the interesting theoretical issue about these higher order non-Gaussianities is an inequality between f_{NL} and τ_{NL} , so-called, Suyama-Yamaguchi inequality [7–9]. If the equality $\tau_{\text{NL}} = 36f_{\text{NL}}^2/25$ is justified, the primordial curvature perturbations should be sourced from a single scalar field. The case with $\tau_{\text{NL}} > 36f_{\text{NL}}^2/25$ indicates that the primordial curvature perturbations might be sourced from multi-scalar fields.

*Email: shu"at"icrr.u-tokyo.ac.jp

†Email: taka"at"kmi.nagoya-u.ac.jp

There have been several works about the effects of these higher order parameters g_{NL} and τ_{NL} on the scale-dependency of the bias parameter. In Ref. [10], the authors derive a scale-dependent bias in the case with non-zero g_{NL} and find that g_{NL} gives the same scale-dependency as the case with f_{NL} . They also give a constraint for g_{NL} by using the same data set as in Ref. [3]. For τ_{NL} , although there are not any available constraints, Refs. [11, 12] analytically derive the formulae of the scale-dependent bias with τ_{NL} (Refs. [13, 14] as related works). Numerical analysis for the effects of such higher order non-Gaussianities on LSS has been shown in Refs. [15–18]. However, comparing with f_{NL} case, the precise formulae for g_{NL} and τ_{NL} cases might be less understood.

In this paper, we extend the analysis of the scale-dependent bias in Ref. [4] to the case with higher order non-Gaussianities characterized by the non-linearity parameters τ_{NL} and g_{NL} , by making use of iPT. In terms of iPT, the effects of g_{NL} and τ_{NL} appear in two-loop order contributions and hence we also investigate the other contributions from the higher order loops.

This paper is organized as follows. In the next section, we derive a power spectrum of the biased objects with including the higher order primordial non-Gaussianities, by making use of iPT. In section III, we focus on the leading order contributions of g_{NL} and τ_{NL} , and discuss the scale- and redshift-dependence of the bias parameters. We introduce the stochasticity parameter in order to investigate the inequality between f_{NL} and τ_{NL} . In section IV, we discuss the higher order effects which are linearly proportional to the non-linearity parameters. Section V is devoted to summary and discussions. We plot the figures of this paper with adopting the best fit cosmological parameters taken from WMAP 7-year data [2].

II. POWER SPECTRUM OF THE BIASED OBJECTS WITH THE PRIMORDIAL NON-GAUSSIANITIES

Here, we focus on the local-type primordial non-Gaussianity because the several literatures have shown that other types of non-Gaussianities such as equilateral-, orthogonal- and folded-types are not so effective on the structure formation of the Universe, compared with the local type.

A. Local-type non-Gaussianity

Let us introduce the local-type non-linearity parameters. The primordial non-Gaussianities of the curvature perturbations, Φ , are usually characterized by the higher order spectra as

$$\begin{aligned}\langle \Phi(\mathbf{k})\Phi(\mathbf{k}') \rangle &= (2\pi)^3 \delta^{(3)}(\mathbf{k} + \mathbf{k}') P_{\Phi}(k), \\ \langle \Phi(\mathbf{k}_1)\Phi(\mathbf{k}_2)\Phi(\mathbf{k}_3) \rangle &= (2\pi)^3 \delta^{(3)}(\mathbf{k}_1 + \mathbf{k}_2 + \mathbf{k}_3) B_{\Phi}(\mathbf{k}_1, \mathbf{k}_2, \mathbf{k}_3), \\ \langle \Phi(\mathbf{k}_1)\Phi(\mathbf{k}_2)\Phi(\mathbf{k}_3)\Phi(\mathbf{k}_4) \rangle_c &= (2\pi)^3 \delta^{(3)}(\mathbf{k}_1 + \mathbf{k}_2 + \mathbf{k}_3 + \mathbf{k}_4) T_{\Phi}(\mathbf{k}_1, \mathbf{k}_2, \mathbf{k}_3, \mathbf{k}_4),\end{aligned}\tag{1}$$

where a index, c , denotes a connected part of the correlation functions. For the local-type case, the higher order spectra are parameterized as

$$\begin{aligned}B_{\Phi}(k_1, k_2, k_3) &= 2f_{\text{NL}} [P_{\Phi}(k_1)P_{\Phi}(k_2) + P_{\Phi}(k_2)P_{\Phi}(k_3) + P_{\Phi}(k_3)P_{\Phi}(k_1)], \\ T_{\Phi}(k_1, k_2, k_3, k_4) &= 6g_{\text{NL}} [P_{\Phi}(k_1)P_{\Phi}(k_2)P_{\Phi}(k_3) + 3 \text{ perms.}] \\ &\quad + \frac{25}{9}\tau_{\text{NL}} [P_{\Phi}(k_1)P_{\Phi}(k_2)P_{\Phi}(|\mathbf{k}_1 + \mathbf{k}_3|) + 11 \text{ perms.}].\end{aligned}\tag{2}$$

In the above expression, we call scale-independent parameters, f_{NL} , g_{NL} and τ_{NL} , as the local-type non-linearity parameters. As the simplest local-type model, we consider that the primordial fluctuations are expanded as

$$\Phi(\mathbf{x}) = \Phi_{\text{G}} + f_{\text{NL}} (\Phi_{\text{G}}(\mathbf{x})^2 - \langle \Phi_{\text{G}}(\mathbf{x})^2 \rangle) + g_{\text{NL}} \Phi_{\text{G}}(\mathbf{x})^3 + \cdots,\tag{3}$$

where Φ_{G} denotes pure Gaussian fluctuations. We have a special inequality for the local-type non-Gaussianity which is given by [7–9]

$$\tau_{\text{NL}} \geq \frac{36}{25} f_{\text{NL}}^2.\tag{4}$$

For the case where the primordial curvature fluctuations are sourced from the quantum fluctuations of a single scalar field and Φ is given by Eq. (3), we can realize the equality of the above relation. If there exist the multiple scalar fields in the early Universe, which are seeds of the primordial curvature fluctuations, we have $\tau_{\text{NL}} > 36/25 f_{\text{NL}}^2$. For example, in the case with

$$\Phi = \phi_{\text{G}}(\mathbf{x}) + \psi_{\text{G}}(\mathbf{x}) + f_{\text{NL}}^{\phi} (\phi_{\text{G}}(\mathbf{x})^2 - \langle \phi_{\text{G}}(\mathbf{x})^2 \rangle), \quad (5)$$

we have

$$f_{\text{NL}} = \frac{f_{\text{NL}}^{\phi}}{(1 + \xi)^2}, \quad \tau_{\text{NL}} = \frac{36}{25} \frac{(f_{\text{NL}}^{\phi})^2}{(1 + \xi)^3}, \quad (6)$$

and

$$\begin{aligned} \tau_{\text{NL}} &= \frac{36}{25} (1 + \xi) f_{\text{NL}}^2 \\ &> \frac{36}{25} f_{\text{NL}}^2, \quad (\text{for } \xi > 0) \end{aligned} \quad (7)$$

where we have used $\langle \phi\psi \rangle = 0$ and $\xi \equiv P_{\psi}/P_{\phi}$ with $P_i (i = \phi, \psi)$ being the power spectrum of each component. Hence, because of this fact, it is important to investigate the relation between τ_{NL} and f_{NL} for studying the origin of the primordial fluctuations.

B. The power spectrum of the biased objects in integrated perturbation theory

Let us derive a formula of the power spectrum of the biased objects with the primordial non-Gaussianity by making use of iPT. Following Refs. [1, 4], we introduce multipoint propagators $\Gamma_X^{(n)}$ of the biased objects X in "Eulerian" space which is given by

$$\langle \frac{\delta^n \delta_X(\mathbf{k})}{\delta \delta_{\text{L}}(\mathbf{k}_1) \cdots \delta \delta_{\text{L}}(\mathbf{k}_n)} \rangle = (2\pi)^{3-3n} \delta^{(3)}(\mathbf{k}_1 + \cdots + \mathbf{k}_n - \mathbf{k}) \Gamma_X^{(n)}(\mathbf{k}_1, \cdots, \mathbf{k}_n), \quad (8)$$

where $\delta_{\text{L}}(\mathbf{k})$ and $\delta_X(\mathbf{k})$ are respectively the Fourier transforms of the linear density field and the number density field of the biased objects in "Eulerian" space. The linear density field $\delta_{\text{L}}(\mathbf{k})$ is given by

$$\delta_{\text{L}}(\mathbf{k}) = \mathcal{M}(k) \Phi(\mathbf{k}). \quad (9)$$

Here, the proportional factor $\mathcal{M}(k)$ is given by

$$\mathcal{M}(k) = \frac{2}{3} \frac{D(z)}{D(z_*)(1 + z_*)} \frac{k^2 T(k)}{H_0^2 \Omega_{\text{m}0}}, \quad (10)$$

where $T(k)$, $D(z)$, H_0 and $\Omega_{\text{m}0}$ are respectively the transfer function, the linear growth factor, the Hubble's constant and the matter density parameter. Here z_* denotes an arbitrary redshift in the matter-dominated era.

The power-, bi- and tri- spectra of $\delta_{\text{L}}(\mathbf{k})$ are respectively given by

$$\begin{aligned} P_{\text{L}}(k) &= \mathcal{M}(k)^2 P_{\Phi}(k), \\ B_{\text{L}}(\mathbf{k}_1, \mathbf{k}_2, \mathbf{k}_3) &= \mathcal{M}(k_1) \mathcal{M}(k_2) \mathcal{M}(k_3) B_{\Phi}(\mathbf{k}_1, \mathbf{k}_2, \mathbf{k}_3), \\ T_{\text{L}}(\mathbf{k}_1, \mathbf{k}_2, \mathbf{k}_3, \mathbf{k}_4) &= \mathcal{M}(k_1) \mathcal{M}(k_2) \mathcal{M}(k_3) \mathcal{M}(k_4) T_{\Phi}(\mathbf{k}_1, \mathbf{k}_2, \mathbf{k}_3, \mathbf{k}_4). \end{aligned} \quad (11)$$

Up to the leading order of the non-linearity parameters f_{NL} , g_{NL} and τ_{NL} , in terms of the multipoint propagators, the power spectrum of the biased objects is given by

$$\begin{aligned} P_X(k) &= \left[\Gamma_X^{(1)}(\mathbf{k}) \right]^2 P_{\text{L}}(k) + \Gamma_X^{(1)}(\mathbf{k}) \int \frac{d^3 p}{(2\pi)^3} \Gamma_X^{(2)}(\mathbf{p}, \mathbf{k} - \mathbf{p}) B_{\text{L}}(\mathbf{k}, -\mathbf{p}, -\mathbf{k} + \mathbf{p}) \\ &\quad + \frac{1}{3} \Gamma_X^{(1)}(\mathbf{k}) \int \frac{d^3 p_1 d^3 p_2}{(2\pi)^6} \Gamma_X^{(3)}(\mathbf{p}_1, \mathbf{p}_2, \mathbf{k} - \mathbf{p}_1 - \mathbf{p}_2) T_{\text{L}}(\mathbf{k}, -\mathbf{p}_1, -\mathbf{p}_2, -\mathbf{k} + \mathbf{p}_1 + \mathbf{p}_2) \end{aligned}$$

$$+\frac{1}{4}\int\frac{d^3p_1d^3p_2}{(2\pi)^6}\Gamma_X^{(2)}(\mathbf{p}_1,\mathbf{k}-\mathbf{p}_1)\Gamma_X^{(2)}(-\mathbf{p}_2,-\mathbf{k}+\mathbf{p}_2)T_L(\mathbf{p}_1,\mathbf{k}-\mathbf{p}_1,-\mathbf{p}_2,-\mathbf{k}+\mathbf{p}_2). \quad (12)$$

While the first line in the above equation has been already obtained and investigated in details in Ref. [4], here, we look more deeply into the second and third lines.

The multipoint propagators include the non-linear evolution of the matter density field and also the bias functions. In order to derive a more useful expression for the power spectrum, let us introduce renormalized bias function in "Lagrangian" space following Ref. [4], which is defined as

$$c_n^L(\mathbf{k}_1, \mathbf{k}_2, \dots, \mathbf{k}_n) = (2\pi)^{3n} \int \frac{d^3p}{(2\pi)^3} \langle \frac{\delta^n \delta_X^L(\mathbf{p})}{\delta \delta_L(\mathbf{k}_1) \dots \delta \delta_L(\mathbf{k}_n)} \rangle, \quad (13)$$

where δ_X^L is the number density field of the biased objects in "Lagrangian" space. The multipoint propagators of the biased objects on large scales ($\mathbf{k}_1 + \mathbf{k}_2 + \dots + \mathbf{k}_n \rightarrow 0$), where the non-linear evolution of the matter density field is negligible, are written in terms of c_n^L as

$$\begin{aligned} \Gamma_X^{(1)}(\mathbf{k}) &\rightarrow 1 + c_1^L(\mathbf{k}), \\ \Gamma_X^{(n)}(\mathbf{k}_1, \mathbf{k}_2, \dots, \mathbf{k}_n) &\rightarrow c_n^L(\mathbf{k}_1, \mathbf{k}_2, \dots, \mathbf{k}_n) \text{ for } n \geq 2. \end{aligned} \quad (14)$$

From Eq. (13), the renormalized bias function is calculated once the relation between the linear density field and the number density field of the biased objects in "Lagrangian" space is determined. Based on the Press-Schechter (PS) picture, the mass function is determined by the probability that the value of the "smoothed" linear density field over mass scale M exceeds a critical value δ_c , denoted by $P(M, \delta_c)$. The smoothed linear density field over mass scale M is given by

$$\delta_M = \int \frac{d^3k}{(2\pi)^3} e^{i\mathbf{k}\cdot\mathbf{x}} W(kR) \delta_L(\mathbf{k}), \quad (15)$$

where R is a comoving scale corresponding to the mass scale M and $W(kR)$ is a usual top-hat window function. Following Ref. [4], the renormalized bias function can be written as

$$c_n^L(\mathbf{k}_1, \dots, \mathbf{k}_n) = \frac{(-1)^n \frac{\partial}{\partial M} \left[\frac{\partial^n P(M, \delta_c)}{\partial \delta_c^n} W(k_1 R) \dots W(k_n R) \right]}{\partial P(M, \delta_c) / \partial M}. \quad (16)$$

Assuming a universal mass function, we have

$$\begin{aligned} \frac{\partial P(M, \delta_c)}{\partial M} &= \frac{f_{\text{MF}}(\nu)}{2} \frac{d \ln \sigma_M}{dM}, \\ \frac{\partial^n P(M, \delta_c)}{\partial \delta_c^n} &= \frac{(-1)^n (n-1)!}{2\delta_c^n} \sum_{m=0}^{n-1} \frac{(-1)^m}{m!} \nu^m f_{\text{MF}}^{(m)}(\nu), \end{aligned} \quad (17)$$

where $f_{\text{MF}}(\nu)$ with $\nu = \delta_c / \sigma_M$ is a multiplicity function. Then, using the above expressions, the renormalized bias functions are reduced to

$$\begin{aligned} c_n^L(k_1, \dots, k_n) &= \frac{(n-1)!}{\delta_c^n f_{\text{MF}}(\nu)} \frac{d}{d \ln \sigma_M} \left[\left(\sum_{m=0}^{n-1} \frac{(-1)^m}{m!} \nu^m f_{\text{MF}}^{(m)}(\nu) \right) W(k_1 R) \dots W(k_n R) \right] \\ &= b_n^L(M) W(k_1 R) \dots W(k_n R) \\ &\quad + \frac{(n-1)!}{\delta_c^n} \left(\sum_{m=0}^{n-1} \frac{\delta_c^m}{m!} b_m^L(M) \right) \frac{d}{d \ln \sigma_M} [W(k_1 R) \dots W(k_n R)], \end{aligned} \quad (18)$$

where the scale independent function, $b_n^L(M)$, given by

$$b_n^L(M) = \left(\frac{-1}{\sigma_M} \right)^n \frac{f_{\text{MF}}^{(n)}(\nu)}{f_{\text{MF}}(\nu)}. \quad (19)$$

We can take into account the effect of the primordial non-Gaussianity on the renormalized bias function by using the non-Gaussian multiplicity function. We discuss the non-Gaussian corrections to the renormalized bias function in a later section. For example, we have

$$f_{\text{MF}}(\nu) = f_{\text{PS}}(\nu) = \sqrt{\frac{2}{\pi}} \nu e^{-\nu^2/2}, \quad (20)$$

in the original PS theory, and

$$f_{\text{MF}}(\nu) = f_{\text{ST}}(\nu) = A(p) \sqrt{\frac{2}{\pi}} \left[1 + \frac{1}{(q\nu^2)^p} \right] \sqrt{q} \nu e^{-q\nu^2/2}, \quad (21)$$

for the Sheth-Tormen (ST) fitting formula with $p = 0.3$, $q = 0.707$ and $A(p) = [1 + \pi^{-1/2} 2^{-p} \Gamma(1/2 - p)]^{-1}$.

III. SCALE-DEPENDENT BIAS WITH PRIMORDIAL NON-GAUSSIANITIES

Here, by using the simple expressions for the multipoint propagators on large scales, which are given in the previous section, let us write down the bias parameter with respect to the non-linearity parameters f_{NL} , g_{NL} and τ_{NL} . Defining a bias parameter as

$$P_X(k) \equiv b_X^2(k) P_L(k), \quad (22)$$

on large scales ($k \rightarrow 0$), we have

$$\begin{aligned} b_X^2(k) &\approx b_1(M)^2 + \Delta b_X^2(k) \\ \Delta b_X^2(k) &\equiv 4f_{\text{NL}} \frac{b_1(M)}{\mathcal{M}(k)} \int \frac{d^3 p_1}{(2\pi)^3} c_2^{\text{L}}(-\mathbf{p}_1, \mathbf{p}_1) P_L(p_1) \\ &\quad + \left(6g_{\text{NL}} + \frac{50}{9} \tau_{\text{NL}} \right) \frac{b_1(M)}{\mathcal{M}(k)} \int \frac{d^3 p_1 d^3 p_2}{(2\pi)^6} \\ &\quad \times c_3^{\text{L}}(-\mathbf{p}_1, -\mathbf{p}_2, \mathbf{p}_1 + \mathbf{p}_2) \mathcal{M}(p_1) \mathcal{M}(p_2) \mathcal{M}(|\mathbf{p}_1 + \mathbf{p}_2|) P_\Phi(p_1) P_\Phi(p_2) \\ &\quad + \frac{25}{9} \tau_{\text{NL}} \frac{1}{\mathcal{M}(k)^2} \int \frac{d^3 p_1 d^3 p_2}{(2\pi)^6} c_2^{\text{L}}(\mathbf{p}_1, -\mathbf{p}_1) c_2^{\text{L}}(\mathbf{p}_2, -\mathbf{p}_2) P_L(p_1) P_L(p_2). \end{aligned} \quad (23)$$

where $b_1(M) \equiv 1 + c_1^{\text{L}}$ is the scale-independent Eulerian linear bias parameter and $\Delta b_X^2(k)$ denotes a scale-dependent part due to the primordial non-Gaussianity. The renormalized bias functions up to the third order are given by

$$\begin{aligned} c_2^{\text{L}}(-\mathbf{p}_1, \mathbf{p}_1) &= b_2^{\text{L}}(M) W(p_1 R)^2 + 2 \frac{1 + \delta_c (b_1(M) - 1)}{\delta_c^2} W(p_1 R) \frac{dW(p_1 R)}{d \ln \sigma_M}, \\ c_3^{\text{L}}(-\mathbf{p}_1, -\mathbf{p}_2, \mathbf{p}_1 + \mathbf{p}_2) &= b_3^{\text{L}}(M) W(p_1 R) W(p_2 R) W(|\mathbf{p}_1 + \mathbf{p}_2| R) \\ &\quad + \frac{2 + 2\delta_c (b_1(M) - 1) + \delta_c^2 b_2^{\text{L}}(M)}{\delta_c^3} \frac{d}{d \ln \sigma_M} [W(p_1 R) W(p_2 R) W(|\mathbf{p}_1 + \mathbf{p}_2| R)]. \end{aligned} \quad (24)$$

Substituting these expressions into Eq. (23), we have

$$\begin{aligned} \Delta b_X^2(k) &\approx 4f_{\text{NL}} \frac{b_1(M)}{\mathcal{M}(k)} \left[b_2^{\text{L}}(M) + 2 \frac{1 + \delta_c (b_1(M) - 1)}{\delta_c^2} \right] \sigma_M^2 \\ &\quad + \left(g_{\text{NL}} + \frac{25}{27} \tau_{\text{NL}} \right) \frac{b_1(M)}{\mathcal{M}(k)} \\ &\quad \times \left[b_3^{\text{L}}(M) + \frac{2 + 2\delta_c (b_1(M) - 1) + \delta_c^2 b_2^{\text{L}}(M)}{\delta_c^3} \left(4 + \frac{d \ln S_3(M)}{\ln \sigma_M} \right) \right] \sigma_M^4 S_3(M) \\ &\quad + \frac{25}{9} \tau_{\text{NL}} \frac{1}{\mathcal{M}(k)^2} \left[b_2^{\text{L}}(M) + 2 \frac{1 + \delta_c (b_1(M) - 1)}{\delta_c^2} \right]^2 \sigma_M^4, \end{aligned} \quad (25)$$

where σ_M is a variance of the smoothed density field, δ_M , and $S_3(M)$ is a skewness given by

$$S_3(M) = \frac{6}{\sigma_M^4} \int \frac{d^3 p_1 d^3 p_2}{(2\pi)^6} W(p_1 R) W(p_2 R) W(|\mathbf{p}_1 + \mathbf{p}_2| R) \mathcal{M}(p_1) \mathcal{M}(p_2) \mathcal{M}(|\mathbf{p}_1 + \mathbf{p}_2|) P_\Phi(p_1) P_\Phi(p_2). \quad (26)$$

The first line in the above expression has been already shown in Ref. [4] and gives the scale-dependence with $\Delta b(k) \propto 1/k^2$. A recent paper by Biagetti, Desjacques and Riotto (2012) [14] have shown a non-Gaussian correction to the bias including the effect of τ_{NL} and we find that their expression of the non-Gaussian correction coincides with the second line in our Eq. (25), by employing the PS mass function. Gong and Yokoyama (2011) [11] derived the similar correction term dependent on τ_{NL} as the last term in Eq. (25) by making use of the high peak limit formalism. By employing PS mass function and taking high peak limit, we find that the last term in our expression would agree with the τ_{NL} -correction term in Ref. [11]. In this sense that the results in the previous works are included in Eq. (25) as limiting expressions, this expression is a general expression of the scale-dependent bias depending on the non-linearity parameters, f_{NL} , g_{NL} and τ_{NL} .

A. f_{NL} vs g_{NL}

Let us focus on g_{NL} -correction term. From Eq. (25), we find the g_{NL} -correction gives the same scale-dependence as the f_{NL} -correction. In this sense, the non-linearity parameters g_{NL} and f_{NL} are degenerate with each other in the observation of the biased objects. One way to distinguish these two non-linearity parameters is to see the mass-dependence ($b_1(M)$ -dependence) of the non-Gaussian corrections, which has been shown in Ref. [18]. Here, we focus on the redshift-dependence at fixed scale of the non-Gaussian corrections. In Fig. 1, we plot Δb as functions of the redshift with fixing $k = 0.01 \, h \, \text{Mpc}^{-1}$ and $M = 5 \times 10^{13} \, h^{-1} M_\odot$. We set $f_{\text{NL}} = 40$ for red circles and $g_{\text{NL}} = 5 \times 10^5$ for blue boxes. From this figure, we find that the redshift dependence of the scale-dependent part of the bias parameter

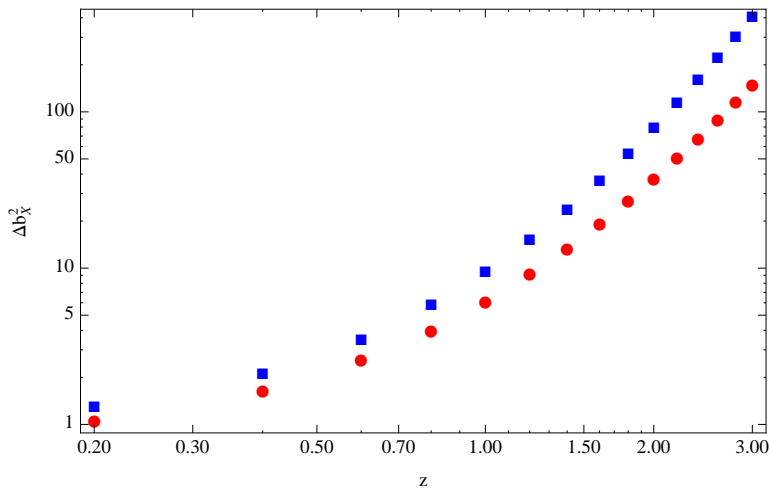


FIG. 1: Δb_X^2 as functions of the redshift with fixing $k = 0.005 \, h \, \text{Mpc}^{-1}$ and $M = 5 \times 10^{13} \, h^{-1} M_\odot$. We set $f_{\text{NL}} = 40$ for red circles and $g_{\text{NL}} = 5 \times 10^5$ for blue boxes.

is different between the cases with non-zero f_{NL} and g_{NL} , and also we can see that the higher redshift observations would be a powerful tool to obtain a constraint for g_{NL} .

B. f_{NL} vs τ_{NL}

Next, let us focus on the τ_{NL} -correction terms. As we have mentioned, a significant constraint on the τ_{NL} parameter is a powerful probe of the origins of the primordial adiabatic fluctuations, since it has a special inequality with f_{NL} . To focus on the inequality between f_{NL} and τ_{NL} in the context of the scale-dependent bias, we introduce the power spectrum of the matter density field, P_m , and also the cross power spectrum, P_{mX} . On large scales where the

non-linear evolution of the matter density field is negligible, these power spectra are approximately written as

$$\begin{aligned}
P_m(k) &\approx P_L(k), \\
P_{mX}(k) &\approx b_1(M)P_L(k) + 2f_{\text{NL}} \frac{P_L(k)}{\mathcal{M}(k)} \int \frac{d^3 p_1}{(2\pi)^3} c_2^{\text{L}}(-\mathbf{p}_1, \mathbf{p}_1) P_L(p_1) \\
&\quad + \left(3g_{\text{NL}} + \frac{25}{9}\tau_{\text{NL}} \right) \frac{P_L(k)}{\mathcal{M}(k)} \int \frac{d^3 p_1 d^3 p_2}{(2\pi)^6} \\
&\quad \times c_3^{\text{L}}(-\mathbf{p}_1, -\mathbf{p}_2, \mathbf{p}_1 + \mathbf{p}_2) \mathcal{M}(p_1) \mathcal{M}(p_2) \mathcal{M}(|\mathbf{p}_1 + \mathbf{p}_2|) P_\Phi(p_1) P_\Phi(p_2).
\end{aligned} \tag{27}$$

By making use of the matter power spectrum and the cross power spectrum, we estimate a stochasticity (see, e.g.,

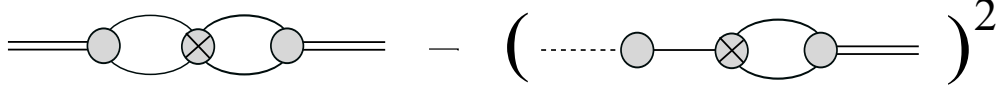


FIG. 2: The diagrammatic picture for the stochasticity parameter $\tilde{r}(k) - 1$. The double solid line, the dashed line, the solid line and the circle represent respectively δ_X , δ_m , δ_L and the multipoint propagator.

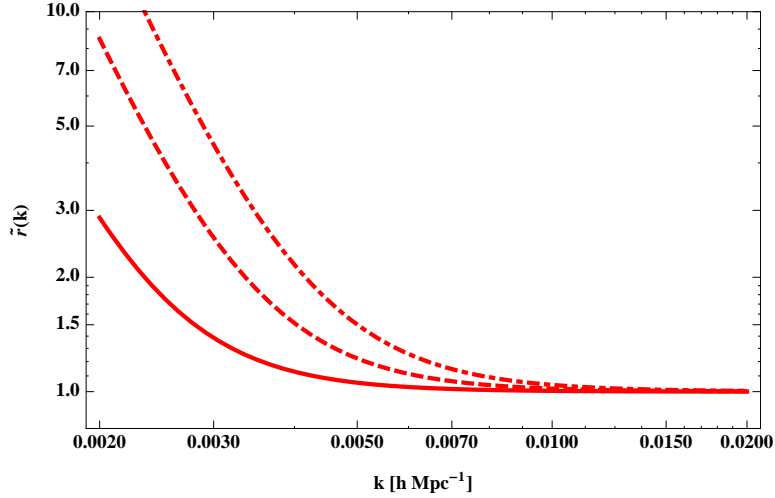


FIG. 3: The stochasticity parameter as a function of k with fixing $z = 1$, $M = 5 \times 10^{13} h^{-1} M_\odot$ and $f_{\text{NL}} = 40$. The red thick line is for the case with $\tau_{\text{NL}} = 2 \times 36 f_{\text{NL}}^2 / 25$. The red dashed line is for $\tau_{\text{NL}} = 5 \times 36 f_{\text{NL}}^2 / 25$ and the red dotted-dashed line for $\tau_{\text{NL}} = 10 \times 36 f_{\text{NL}}^2 / 25$.

[1, 19, 20]). Here, for convenience, we define a stochasticity parameter as ¹

$$\tilde{r}(k) \equiv \frac{P_m(k) P_X(k)}{P_{mX}(k)^2}. \tag{28}$$

At the leading order, we can obtain

$$\tilde{r}(k) \simeq 1 + \left(\frac{25}{9} \tau_{\text{NL}} - 4 f_{\text{NL}}^2 \right) \frac{1}{b_1(k)^2 \mathcal{M}(k)^2} \left[\int \frac{d^3 p}{(2\pi)^3} c_2^{\text{L}}(\mathbf{p}, -\mathbf{p}) P_L(p) \right]^2. \tag{29}$$

¹ In Refs. [1, 19, 20], the stochasticity parameter is defined as $r(k) \equiv P_{mX}(k) / \sqrt{P_m(k) P_X(k)}$. In Ref. [15], the authors introduce $r(k) \equiv P_X(k) / P_m(k) - (P_{mX}(k) / P_m(k))^2$ and Ref. [13] gives $\chi(k) \equiv P_{mX}(k)^2 / (P_X(k) P_m(k))$. Note that these parameters have the similar dependence on the non-linearity parameters although each definition is slightly different.

The diagrammatic picture of the stochasticity parameter $\tilde{r}(k) - 1$ is shown in Fig. 2, following the rules given in Ref. [1]. In this figure, the double solid line, the dashed line, the solid line and the circle represent respectively δ_X , δ_m , δ_L and the multipoint propagator. In Fig. 3, we plot the stochasticity parameter as a function of the wavenumber, k , with fixing $z = 1$, $M = 5 \times 10^{13} h^{-1} M_\odot$ and $f_{\text{NL}} = 40$. The red thick line is for the case with $\tau_{\text{NL}} = 2 \times 36 f_{\text{NL}}^2 / 25$. The red dashed line is for $\tau_{\text{NL}} = 5 \times 36 f_{\text{NL}}^2 / 25$ and the red dotted-dashed line for $\tau_{\text{NL}} = 10 \times 36 f_{\text{NL}}^2 / 25$. From this figure, we find that due to the deviation from the equality as $\tau_{\text{NL}} = 36 f_{\text{NL}}^2 / 25$ the stochasticity parameter $\tilde{r}(k)$ deviates from unity on large scales. This means that the observations of the stochasticity parameter on large scales could be a powerful tool to study the inequality between f_{NL} and τ_{NL} . This fact was also discussed in Ref. [13, 15] for two-field inflation model with different parameterization. Note that the stochasticity includes various uncertainties due to the higher order corrections [1] and also astrophysical processes. The above discussion about the stochasticity given by Eq. (29) is ideal and hence the detection of the effect of τ_{NL} needs more careful investigation. In later section, we discuss the higher order corrections into the stochasticity.

IV. HIGHER ORDER CORRECTIONS

In the context of the iPT, the correction terms from the non-zero g_{NL} and τ_{NL} discussed in the previous section are two-loop order corrections, while the f_{NL} -correction term is the one-loop order. Of course, we have other higher order corrections which we have neglected in the previous section. Although it is difficult to check all the contributions analytically, in the large scale limit where the non-linear evolution of the matter density field is negligible, the estimation for such contributions becomes somewhat easier. Here, as the higher order corrections, we focus on the corrections in the pure Gaussian fluctuations and also those which are linearly proportional to the non-linearity parameters and discuss in what case we do not need carefully to treat such higher order corrections.

A. Non-Gaussian corrections in multipoint propagators

As we have discussed, the multipoint propagators on large scales are rewritten in terms of the renormalized bias function as Eq. (14) and the renormalized bias functions are given by Eq. (18) in terms of the multiplicity function, $f_{\text{MF}}(\nu)$. In case the primordial non-Gaussianity exists, it has been known that the multiplicity function is modified (see, e.g., Ref. [16]) and hence the multipoint propagators should be also dependent on the non-linearity parameters. To include the corrections due to the primordial non-Gaussianity, we introduce a correction function as R^{NG} and rewrite the multiplicity functions as $f_{\text{MF}} = f_{\text{PS(ST)}} \times R^{\text{NG}}$. There are several works about R^{NG} analytically and numerically. For example, based on the Edgeworth expansion formula, up to the terms which are linearly proportional to the non-linearity parameters, we have

$$R_{\text{Ed}}^{\text{NG}} \simeq 1 + \left(\frac{\kappa_3(M)}{6} H_3(\nu) + \frac{1}{\nu} \frac{\partial \kappa_3(M)/\partial M}{6 \partial \ln \sigma_M / \partial M} H_2(\nu) \right) + \left(\frac{\kappa_4(M)}{24} H_4(\nu) + \frac{1}{\nu} \frac{\partial \kappa_4(M)/\partial M}{24 \partial \ln \sigma_M / \partial M} H_3(\nu) \right), \quad (30)$$

with $\kappa_n = \langle \delta_R^n \rangle_c / \sigma_M^n$ and $H_n(x)$ being Hermite polynomial. The higher order moments κ_3 and κ_4 are respectively proportional to the non-linearity parameters f_{NL} and g_{NL} (also τ_{NL}). As another example, Matarrese, Verde and Jimenez (2000) [21] has shown a fitting formula for R_{NL} which is given by

$$R_{\text{MVJ}}^{\text{NG}} = \left[\delta_3 - \frac{\nu}{\delta_3} \frac{\kappa_3(M)}{6} - \frac{\partial \kappa_3(M)/\partial M}{6 \partial \ln \sigma_M / \partial M} \right] \left[\delta_4 - \frac{\nu^2}{\delta_4} \frac{\kappa_4(M)}{12} - \frac{\partial \kappa_4(M)/\partial M}{24 \partial \ln \sigma_M / \partial M} \right] \exp \left[\frac{\kappa_3(M)}{6} \nu^3 + \frac{\kappa_4(M)}{24} \nu^4 \right], \quad (31)$$

with $\delta_n = \sqrt{1 - 2\nu^{n-2} \kappa_n(M)/n!}$.

Let us evaluate the amplitudes of the modifications of the renormalized bias functions due to the primordial non-Gaussianity. Hereinafter, we adopt the Sheth-Tormen fitting formula as a Gaussian mass function and the Edgeworth expansion formula as a non-Gaussian correction of the mass function. In this case, the first order renormalized bias function on large scales ($k \rightarrow 0$) is

$$\begin{aligned} c_{1,\text{NG}}^{\text{L}}(k) &\approx b_{1,\text{NG}}^{\text{L}}(M) = \left(\frac{-1}{\sigma_M} \right) \frac{f'_{\text{MF}}(\nu)}{f_{\text{MF}}(\nu)} = \left(\frac{-1}{\sigma_M} \right) \left[\frac{f'_{\text{PS}}(\nu)}{f_{\text{PS}}(\nu)} + \frac{R_{\text{Ed}}^{\text{NG}'}(\nu)}{R_{\text{Ed}}^{\text{NG}}(\nu)} \right] \\ &\simeq \frac{1}{\delta_c} \left[q\nu^2 - 1 + \frac{2p}{1 + (q\nu^2)^p} \right. \\ &\quad \left. - \frac{\kappa_3(M)}{2} (\nu^3 - \nu) - \frac{\kappa_4(M)}{6} (\nu^4 - 3\nu^2) - \frac{1}{6} \frac{\partial \kappa_3(M)}{\partial \ln \sigma_M} \left(\nu + \frac{1}{\nu} \right) - \frac{1}{12} \frac{\partial \kappa_4(M)}{\partial \ln \sigma_M} \nu^2 \right]. \end{aligned} \quad (32)$$

In Fig. 4, we plot the ratio of the bias parameter in Eulerian space $b_1(M) = 1 + c_1^L$ with the primordial non-Gaussianity to that in the Gaussian case, as a function of ν . The red circles are for the $f_{\text{NL}} = 40$ case, the blue boxes for the $g_{\text{NL}} = 5 \times 10^5$ case and the green diamonds for the $\tau_{\text{NL}} = 10 \times (6 \times 40/5)^2$. From this figure, we find that in the range with $1.5 \lesssim \nu \lesssim 4.5$ corresponding to the mass range of the biased objects with $10^{12} \lesssim M/[h^{-1}M_\odot] \lesssim 5 \times 10^{14}$ for $z = 1$, the contribution of the modifications of the mass function by the primordial non-Gaussianity to the bias is negligibly small. For $f_{\text{NL}} = 40$ and $\nu = 4.5$, the effect of the primordial non-Gaussianity is about 4%. For the higher peak objects ($\nu \gtrsim 5$) the effect of the primordial non-Gaussianity is expected to become larger and hence for much higher peak objects we could not ignore the contribution any more. Such kind of non-Gaussian effects can be observationally seen in the number counts of the very massive objects which are minor components in the observations of the clustering of the biased objects.

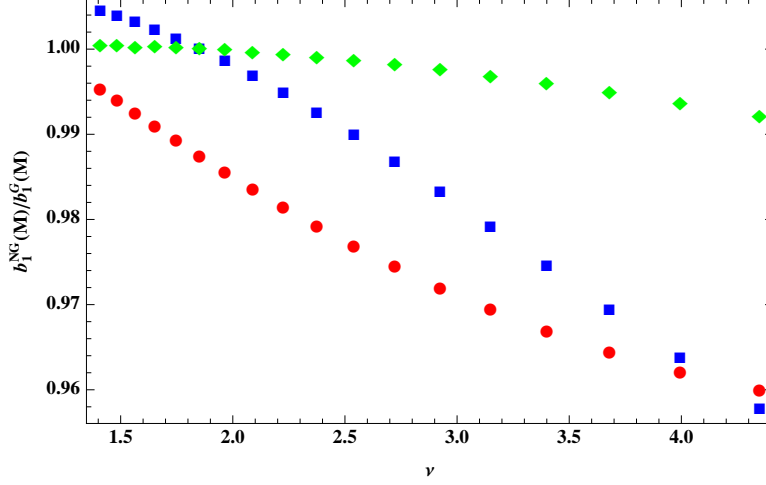


FIG. 4: The ratio between the non-Gaussian first order bias parameter and the Gaussian one, $b_1^{\text{NG}}(M)/b_1^{\text{G}}(M)$ as a function of ν . The red circles are for the $f_{\text{NL}} = 40$ case, the blue boxes for the $g_{\text{NL}} = 5 \times 10^5$ case and the green diamonds for the $\tau_{\text{NL}} = 10 \times (6 \times 40/5)^2$.

B. Higher order loops in terms of the multipoint propagators

In the previous subsection, we find that the modification of the multipoint propagators due to the primordial non-Gaussianity is small for not so high peak objects. Hereinafter, we consider the case with $M = 5 \times 10^{13} h^{-1}M_\odot$ at $z = 1.0$ and neglect the effects of the primordial non-Gaussianity which appear in the multipoint propagators.

Next, let us focus on the higher order loop corrections in the power spectrum of the biased objects, in terms of the multipoint propagators, $\Gamma_X^{(n)}$. The power spectrum of the biased objects, up to the terms which are linearly proportional to the non-linearity parameters, is obtained by

$$\begin{aligned}
 P_X(k) = & \sum_{n=1}^{\infty} \left[\frac{1}{n!} \int \frac{d^3 p_1 \cdots d^3 p_{n-1}}{(2\pi)^{3n}} \Gamma_X^{(n)}(\mathbf{p}_1, \mathbf{p}_2, \dots, \mathbf{k} - \mathbf{P}_{n-1})^2 P_L(p_1) P_L(p_2) \cdots P_L(|\mathbf{k} - \mathbf{P}_{n-1}|) \right. \\
 & + \frac{1}{(n-1)!} \int \frac{d^3 p_1 \cdots d^3 p_n}{(2\pi)^{3n}} \Gamma_X^{(n)}(\mathbf{p}_1, \dots, \mathbf{p}_{n-1}, \mathbf{k} - \mathbf{P}_{n-1}) \\
 & \quad \times \Gamma_X^{(n+1)}(-\mathbf{p}_1, \dots, -\mathbf{p}_n, -\mathbf{k} + \mathbf{P}_n) P_L(p_1) \cdots P_L(p_{n-1}) B_L(\mathbf{k} - \mathbf{P}_{n-1}, -\mathbf{p}_n, -\mathbf{k} + \mathbf{P}_n) \\
 & + \frac{1}{3(n-1)!} \int \frac{d^3 p_1 \cdots d^3 p_{n+1}}{(2\pi)^{3n+3}} \Gamma_X^{(n)}(\mathbf{p}_1, \dots, \mathbf{p}_{n-1}, \mathbf{k} - \mathbf{P}_{n-1}) \\
 & \quad \times \Gamma_X^{(n+2)}(-\mathbf{p}_1, \dots, -\mathbf{p}_{n+1}, -\mathbf{k} + \mathbf{P}_{n+1}) P_L(p_1) \cdots P_L(p_{n-1}) T_L(\mathbf{k} - \mathbf{P}_{n-1}, -\mathbf{p}_n, -\mathbf{p}_{n+1}, -\mathbf{k} + \mathbf{P}_{n+1}) \left. \right] \\
 & + \sum_{n=2}^{\infty} \frac{1}{4(n-2)!} \int \frac{d^3 p_1 \cdots d^3 p_{n-1} d^3 q}{(2\pi)^{3n}} \Gamma_X^{(n)}(\mathbf{p}_1, \dots, \mathbf{p}_{n-1}, \mathbf{k} - \mathbf{P}_{n-1})
 \end{aligned}$$

$$\begin{aligned}
& \times \Gamma_X^{(n)}(-\mathbf{p}_1, \dots, -\mathbf{p}_{n-2}, -\mathbf{q}, -\mathbf{k} + \mathbf{P}_{n-2} + \mathbf{q}) \\
& \times P_L(p_1) \cdots P_L(p_{n-2}) T_L(\mathbf{p}_{n-1}, \mathbf{k} - \mathbf{P}_{n-1}, -\mathbf{q}, -\mathbf{k} + \mathbf{P}_{n-2} + \mathbf{q}),
\end{aligned} \tag{33}$$

where $\mathbf{P}_n = \mathbf{p}_1 + \cdots + \mathbf{p}_n$. In the right hand side of the above equation, the first term in the bracket appears

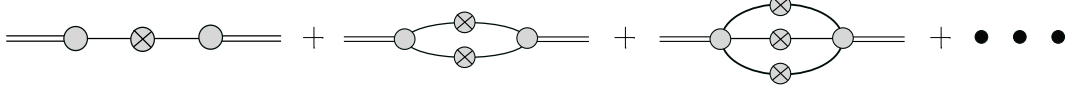


FIG. 5: Pure Gaussian case

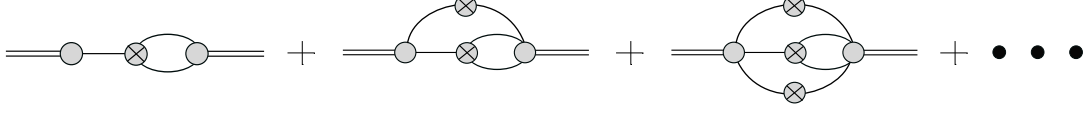


FIG. 6: Diagrams linearly proportional to the primordial bispectrum.

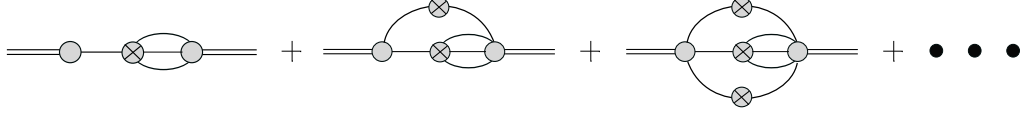


FIG. 7: Diagrams linearly proportional to the primordial trispectrum.

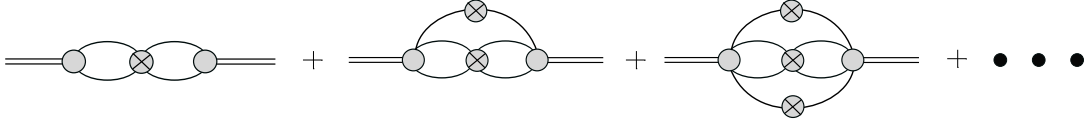


FIG. 8: Other diagrams linearly proportional to the primordial trispectrum.

even in the case with pure Gaussian fluctuations, corresponding to Fig. 5. The second term in the bracket represents the contributions which are linearly proportional to the primordial bispectrum parameterized by f_{NL} . This term is corresponding to Fig. 6. Both the third and last terms are the contributions which are linearly proportional to the primordial trispectrum parameterized by g_{NL} and τ_{NL} . These terms are respectively shown by Figs. 7 and 8. Such kind of higher order corrections for the power spectrum of the matter density fields are estimated by changing $\Gamma_X^{(n)}$ to $\Gamma_m^{(n)}$ in the above expression. As we have mentioned, the non-linearity of the matter density fields becomes negligible and $\Gamma_m^{(1)} \rightarrow 1$ and $\Gamma_m^{(n)} \rightarrow 0$ ($n \geq 2$) on large scales ($k \rightarrow 0$). Hence, for the power spectrum of the matter density fields such higher order correction terms are negligible on large scales.

Using Eq. (14), the power spectrum of the biased objects including the higher order corrections is reduced into

$$\begin{aligned}
P_X(k) & \approx b_1(k)^2 P_L(k) + 4f_{\text{NL}} b_1(k) \frac{P_L(k)}{\mathcal{M}(k)} \int \frac{d^3 p_1}{(2\pi)^3} c_2^L(-\mathbf{p}_1, \mathbf{p}_1) P_L(p_1) \\
& + \left(6g_{\text{NL}} + \frac{50}{9} \tau_{\text{NL}} \right) b_1(k) \frac{P_L(k)}{\mathcal{M}(k)} \int \frac{d^3 p_1 d^3 p_2}{(2\pi)^6} \\
& \quad \times c_3^L(-\mathbf{p}_1, -\mathbf{p}_2, \mathbf{p}_1 + \mathbf{p}_2) \mathcal{M}(p_1) \mathcal{M}(p_2) \mathcal{M}(|\mathbf{p}_1 + \mathbf{p}_2|) P_\Phi(p_1) P_\Phi(p_2) \\
& + \frac{25}{9} \tau_{\text{NL}} \frac{P_L(k)}{\mathcal{M}(k)^2} \int \frac{d^3 p_1 d^3 q}{(2\pi)^6} c_2^L(\mathbf{p}_1, -\mathbf{p}_1) c_2^L(\mathbf{q}, -\mathbf{q}) P_L(p_1) P_L(q) \\
& + P_{\text{const.}},
\end{aligned}$$

$$\begin{aligned}
P_{\text{const.}} = & \sum_{n=2}^{\infty} \frac{1}{n!} \int \frac{d^3 p_1 \cdots d^3 p_{n-1}}{(2\pi)^{3n-3}} c_n^{\text{L}}(\mathbf{p}_1, \mathbf{p}_2, \cdots, -\mathbf{P}_{n-1})^2 P_{\text{L}}(p_1) P_{\text{L}}(p_2) \cdots P_{\text{L}}(|\mathbf{P}_{n-1}|) \\
& + 2f_{\text{NL}} \sum_{n=2}^{\infty} \frac{1}{(n-1)!} \int \frac{d^3 p_1 \cdots d^3 p_n}{(2\pi)^{3n}} c_n^{\text{L}}(\mathbf{p}_1, \cdots, \mathbf{p}_{n-1}, -\mathbf{P}_{n-1}) \\
& \quad \times c_{n+1}^{\text{L}}(-\mathbf{p}_1, \cdots, -\mathbf{p}_n, \mathbf{P}_n) P_{\text{L}}(p_1) \cdots P_{\text{L}}(p_{n-1}) \mathcal{M}(|\mathbf{P}_{n-1}|) \mathcal{M}(p_n) \mathcal{M}(|\mathbf{P}_n|) \\
& \quad \times [2P_{\Phi}(|\mathbf{P}_{n-1}|) P_{\Phi}(p_n) + P_{\Phi}(|\mathbf{P}_n|) P_{\Phi}(p_n)] \\
& + 6g_{\text{NL}} \sum_{n=2}^{\infty} \frac{1}{3(n-1)!} \int \frac{d^3 p_1 \cdots d^3 p_{n+1}}{(2\pi)^{3n+3}} c_n^{\text{L}}(\mathbf{p}_1, \cdots, \mathbf{p}_{n-1}, -\mathbf{P}_{n-1}) \\
& \quad \times c_{n+2}^{\text{L}}(-\mathbf{p}_1, \cdots, -\mathbf{p}_{n+1}, \mathbf{P}_{n+1}) P_{\text{L}}(p_1) \cdots P_{\text{L}}(p_{n-1}) \mathcal{M}(|\mathbf{P}_{n-1}|) \mathcal{M}(p_n) \mathcal{M}(p_{n+1}) \mathcal{M}(|\mathbf{P}_{n+1}|) \\
& \quad \times [3P_{\Phi}(|\mathbf{P}_{n-1}|) P_{\Phi}(p_n) P_{\Phi}(p_{n+1}) + P_{\Phi}(p_n) P_{\Phi}(p_{n+1}) P_{\Phi}(|\mathbf{P}_{n+1}|)] \\
& + \frac{25}{9} \tau_{\text{NL}} \sum_{n=2}^{\infty} \frac{2}{(n-1)!} \int \frac{d^3 p_1 \cdots d^3 p_{n+1}}{(2\pi)^{3n+3}} c_n^{\text{L}}(\mathbf{p}_1, \cdots, \mathbf{p}_{n-1}, -\mathbf{P}_{n-1}) \\
& \quad \times c_{n+2}^{\text{L}}(-\mathbf{p}_1, \cdots, -\mathbf{p}_{n+1}, \mathbf{P}_{n+1}) P_{\text{L}}(p_1) \cdots P_{\text{L}}(p_{n-1}) \mathcal{M}(|\mathbf{P}_{n-1}|) \mathcal{M}(p_n) \mathcal{M}(p_{n+1}) \mathcal{M}(|\mathbf{P}_{n+1}|) \\
& \quad \times [P_{\Phi}(|\mathbf{P}_{n-1}|) P_{\Phi}(p_n) P_{\Phi}(p_{n+1}) + P_{\Phi}(p_n) P_{\Phi}(p_{n+1}) P_{\Phi}(|\mathbf{P}_{n+1}|)] \\
& + 6g_{\text{NL}} \int \frac{d^3 p_1 d^3 q}{(2\pi)^6} c_{2,\text{G}}^{\text{L}}(\mathbf{p}_1, -\mathbf{p}_1) c_{2,\text{G}}^{\text{L}}(-\mathbf{q}, \mathbf{q}) \mathcal{M}(p_1)^2 \mathcal{M}(q)^2 P_{\Phi}(p_1)^2 P_{\Phi}(q) \\
& + 3g_{\text{NL}} \sum_{n=3}^{\infty} \frac{1}{(n-2)!} \int \frac{d^3 p_1 \cdots d^3 p_{n-1} d^3 q}{(2\pi)^{3n}} c_n^{\text{L}}(\mathbf{p}_1, \cdots, \mathbf{p}_{n-1}, -\mathbf{P}_{n-1}) \\
& \quad \times c_n^{\text{L}}(-\mathbf{p}_1, \cdots, -\mathbf{P}_{n-2}, -\mathbf{q}, \mathbf{P}_{n-2} + \mathbf{q}) \mathcal{M}(p_{n-1}) \mathcal{M}(|\mathbf{P}_{n-1}|) \mathcal{M}(q) \mathcal{M}(|\mathbf{P}_{n-2} + \mathbf{q}|) \\
& \quad \times P_{\text{L}}(p_1) \cdots P_{\text{L}}(p_{n-2}) [P_{\Phi}(p_{n-1}) P_{\Phi}(|\mathbf{P}_{n-1}|) P_{\Phi}(q) + P_{\Phi}(p_{n-1}) P_{\Phi}(q) P_{\Phi}(|\mathbf{P}_{n-2} + \mathbf{q}|)] \\
& + \frac{25}{9} \tau_{\text{NL}} \sum_{n=3}^{\infty} \frac{1}{(n-2)!} \int \frac{d^3 p_1 \cdots d^3 p_{n-1} d^3 q}{(2\pi)^{3n}} c_n^{\text{L}}(\mathbf{p}_1, \cdots, \mathbf{p}_{n-1}, -\mathbf{P}_{n-1}) \\
& \quad \times c_n^{\text{L}}(-\mathbf{p}_1, \cdots, -\mathbf{P}_{n-2}, -\mathbf{q}, \mathbf{P}_{n-2} + \mathbf{q}) \mathcal{M}(p_{n-1}) \mathcal{M}(|\mathbf{P}_{n-1}|) \mathcal{M}(q) \mathcal{M}(|\mathbf{P}_{n-2} + \mathbf{q}|) \\
& \quad \times P_{\text{L}}(p_1) \cdots P_{\text{L}}(p_{n-2}) \left[P_{\Phi}(|\mathbf{P}_{n-1}|) P_{\Phi}(p_{n-1}) P_{\Phi}(q) \right. \\
& \quad \left. + P_{\Phi}(p_{n-1}) P_{\Phi}(|\mathbf{P}_{n-1}|) P_{\Phi}(|\mathbf{p}_{n-1} - \mathbf{q}|) + P_{\Phi}(q) P_{\Phi}(|\mathbf{P}_{n-1}|) P_{\Phi}(|\mathbf{p}_{n-1} - \mathbf{q}|) \right]. \tag{34}
\end{aligned}$$

In the above equation, all the higher order correction terms are included in $P_{\text{const.}}$ in large scale limit and $P_{\text{const.}}$ gives the correction in the bias as $\Delta b_{\text{const.}} \equiv P_{\text{const.}}/P_{\text{L}}(k) \propto 1/P_{\text{L}}(k) \propto 1/k$. In the pure Gaussian case ($f_{\text{NL}} = g_{\text{NL}} = \tau_{\text{NL}} = 0$), the correction in the bias $\Delta b_{\text{const.}}/b_X^2$ as a function of $b_1(M)$ is shown in Fig. 9. From this figure, we find that the contributions from the higher order correction terms to the bias parameter are negligible for the objects with not so large mass. In case we consider here, the dimensionless power spectrum of the biased objects, which is given by $k^3 P_X(k)$, is smaller than unity. We could not neglect higher order correction terms any more, when $k^3 P_X(k)$ becomes order of unity, in which we consider the smaller scales (larger k) and the higher peak objects (larger b_X^2). We also plot the two-loop contribution which is linearly proportional to the non-linearity parameter f_{NL} in Fig. 10. In this figure, we plot $|\Delta b_{\text{const.}}/b_X^2|$ with $f_{\text{NL}} = 40$ at $z = 1.0$. We also fix the scale as $k = 0.005 h \text{ Mpc}^{-1}$. This figure also shows that the correction terms linearly proportional to f_{NL} are negligible for the objects with not so large mass. Here we only show the results up to the two-loop order contributions. However, the higher order contributions than three-loops are expected to be small for the case we consider here, because in Fig. 9 the two-loop correction is smaller than the one-loop one. We expect that the contributions from the higher order loops which are linearly proportional to the primordial trispectrum are also much smaller, from the fact that the two-loop f_{NL} -correction is smaller than the Gaussian higher order loop corrections shown in Fig. 10. Of course, for the more precise discussion about the higher order corrections, we need numerical calculations.

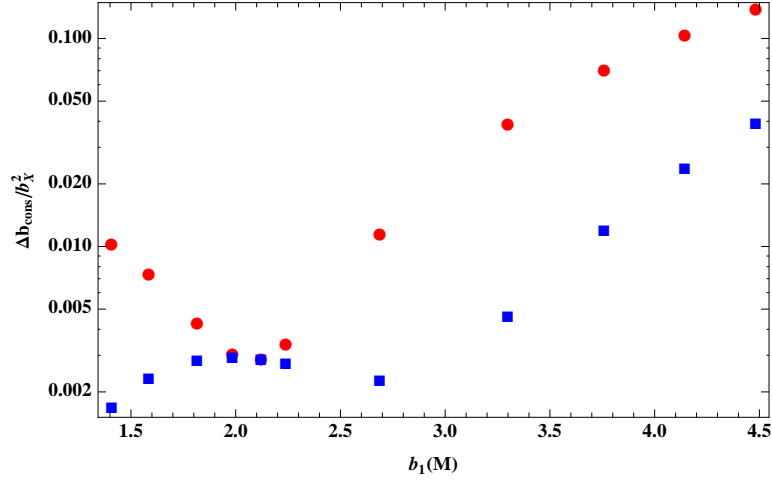


FIG. 9: $\Delta b_{\text{const.}}/b_X^2$ as a function of the Eulerian bias $b_1(M)$ for the pure Gaussian case. We fixed $z = 1.0$ and $k = 0.005 \, h \, \text{Mpc}^{-1}$. The red circles correspond to the one-loop correction and the blue boxes are the two-loop correction.

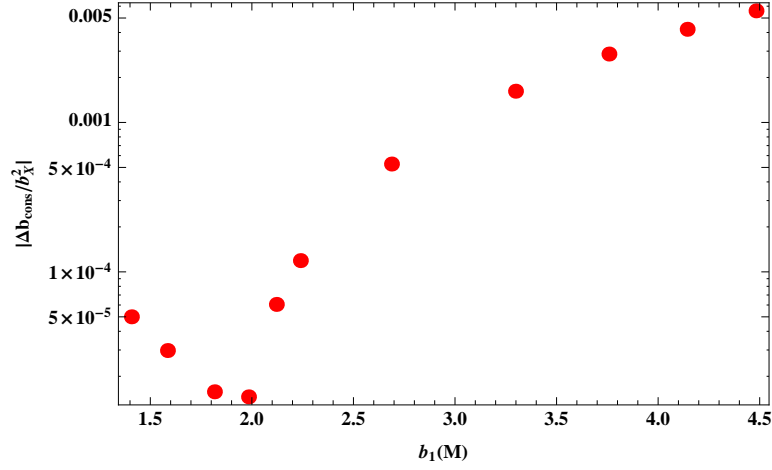


FIG. 10: $|\Delta b_{\text{const.}}/b_X^2|$ as a function of the Eulerian bias $b_1(M)$ with $f_{\text{NL}} = 40$. We fixed $z = 1.0$ and $k = 0.005 \, h \, \text{Mpc}^{-1}$.

Finally, we discuss the contributions of the higher order correction terms in the stochasticity parameter. Ref. [1] have discussed that the one-loop term could generate the stochasticity even in the pure Gaussian case. As we have mentioned in the previous section, the stochasticity parameter would be a powerful tool to test the relation between f_{NL} and τ_{NL} and hence the higher order corrections might become "noises" for the test even on large scales. Based on the expression for the power spectrum of the biased objects given by Eq. (34), which include the higher order corrections, we obtain the stochasticity parameter as

$$\begin{aligned}
 \tilde{r}(k) - 1 \simeq & \left(\frac{25}{9} \tau_{\text{NL}} - 4 f_{\text{NL}}^2 \right) \frac{1}{b_1(k)^2 \mathcal{M}(k)^2} \left[\int \frac{d^3 p}{(2\pi)^3} c_2^{\text{L}}(\mathbf{p}, -\mathbf{p}) P_{\text{L}}(p) \right]^2 \\
 & + \frac{1}{2} \frac{1}{b_1(k)^2 P_{\text{L}}(k)} \left[\int \frac{d^3 p}{(2\pi)^3} c_2^{\text{L}}(\mathbf{p}, -\mathbf{p})^2 P_{\text{L}}(p)^2 \right. \\
 & \quad \left. + \frac{1}{3} \int \frac{d^3 p_1}{(2\pi)^3} \frac{d^3 p_2}{(2\pi)^6} c_3^{\text{L}}(\mathbf{p}_1, \mathbf{p}_2, -\mathbf{p}_1 - \mathbf{p}_2)^2 P_{\text{L}}(p_1) P_{\text{L}}(p_2) P_{\text{L}}(|\mathbf{p}_1 + \mathbf{p}_2|) \right] \\
 & + \frac{2 f_{\text{NL}}}{b_1(k)^2 P_{\text{L}}(k)} \left\{ \int \frac{d^3 p_1 d^3 p_2}{(2\pi)^6} c_2^{\text{L}}(\mathbf{p}_1, -\mathbf{p}_1) c_3^{\text{L}}(\mathbf{p}_1, \mathbf{p}_2, -\mathbf{p}_1 - \mathbf{p}_2) \right\}
 \end{aligned}$$

$$\begin{aligned}
& \times P_L(p_1) \frac{P_L(p_2)}{\mathcal{M}(p_2)} \mathcal{M}(p_1) \mathcal{M}(|\mathbf{p}_1 + \mathbf{p}_2|) [2P_\Phi(p_1) + P_\Phi(|\mathbf{p}_1 + \mathbf{p}_2|)] \\
& - \frac{1}{b_1(k) \mathcal{M}(k)} \int \frac{d^3 p_1}{(2\pi)^3} c_2^L(\mathbf{p}_1, -\mathbf{p}_1)^2 P_L(p_1)^2 \int \frac{d^3 p_2}{(2\pi)^3} c_2^L(\mathbf{p}_2, -\mathbf{p}_2) P_L(p_2) \Big\} \\
& + \frac{6g_{\text{NL}}}{b_1(k)^2 P_L(k)} \int \frac{d^3 p_1}{(2\pi)^3} c_2^L(\mathbf{p}_1, -\mathbf{p}_1) P_L(p_1) P_\Phi(p_1) \int \frac{d^3 p_2}{(2\pi)^3} c_2^L(\mathbf{p}_2, -\mathbf{p}_2) P_L(p_2). \quad (35)
\end{aligned}$$

Here, we consider the contributions up to the two-loop order. In Fig. 11, we plot the contribution of each term to

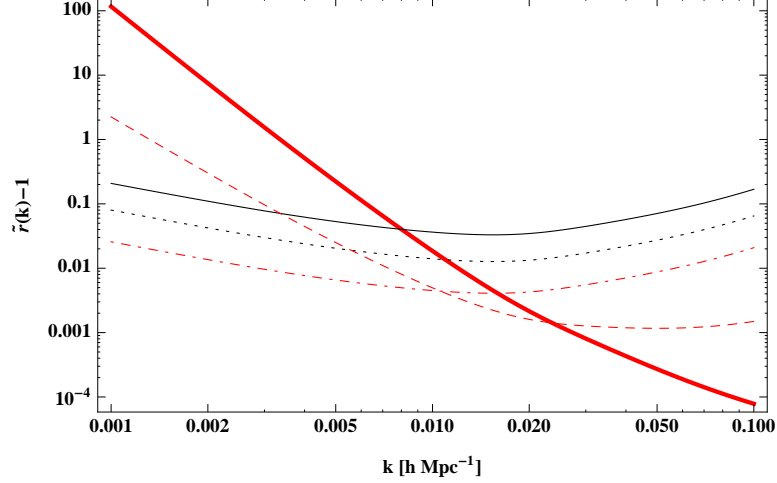


FIG. 11: Contribution of each term to the stochasticity parameter as a function of the wavenumber, k , with fixing $z = 1$ and $M = 5 \times 10^{13} h^{-1} M_\odot$. The red thick line shows the term which is related with the inequality between the non-linearity parameters f_{NL} and τ_{NL} for $f_{\text{NL}} = 40$ and $\tau_{\text{NL}} = 5 \times 36 f_{\text{NL}}^2 / 25$. The black solid and dotted lines are respectively for the one-loop and two-loop contributions which appear even in pure Gaussian case. The red dashed and dotted-dashed lines are for the terms linearly proportional to f_{NL} , which are related with only c_2^L (negative sign term) and c_3^L , respectively..

the stochasticity parameter as a function of the wavenumber k , with fixing $z = 1$ and $M = 5 \times 10^{13} h^{-1} M_\odot$. The red thick line shows the term which is related with the inequality between the non-linearity parameters f_{NL} and τ_{NL} for $f_{\text{NL}} = 40$ and $\tau_{\text{NL}} = 5 \times 36 f_{\text{NL}}^2 / 25$. The black solid and dotted lines are respectively for the one-loop and two-loop contributions which appear even in pure Gaussian case. The red dashed and dotted-dashed lines are for the terms linearly proportional to f_{NL} , which are related with only c_2^L (negative sign term) and c_3^L , respectively. For these parameters, we find that the relation between f_{NL} and τ_{NL} would be observationally checked by large scale survey with $k < O(10^{-2}) h\text{Mpc}^{-1}$. However, as I mentioned before, the stochasticity includes various uncertainties due to other astrophysical processes. The above discussion even including the higher order contributions is still ideal and hence the detection of the effect of τ_{NL} needs more careful investigation.

V. SUMMARY AND DISCUSSION

In this paper, we have derived an accurate formula for the bias parameter with the primordial non-Gaussianity parameterized not only by the non-linearity parameter, f_{NL} , but also by g_{NL} and τ_{NL} , by making use of the iPT. The scale-dependency of the bias induced from g_{NL} is the same as that induced from f_{NL} . In this sense, it is difficult to distinguish the effect of g_{NL} with that of f_{NL} . However, we show that the redshift-dependence of the effect of g_{NL} is different from that of f_{NL} and also to obtain a significant constraint for g_{NL} the higher redshift observations would be invaluable. Recently, as an observation of the biased object at high redshift, an ionized fraction in the reionization era ($6 < z < 20$) through the 21cm observation has been proposed. In Ref. [22, 23], the authors shown that through such kind of the future observations we could obtain a tight constraint for f_{NL} . We expect that such future observation can be also expected to give a tighter constraint for g_{NL} .

For τ_{NL} , there exist a special inequality between f_{NL} and τ_{NL} . We consider the possibility of studying this inequality through the LSS observations and find that the stochasticity parameter deviates from unity in case $\tau_{\text{NL}} > 36 f_{\text{NL}}^2 / 25$. We expect that the future wide field survey would be a powerful tool to obtain a constraint for τ_{NL} .

In deriving the formula with the primordial non-Gaussianity parameterized by g_{NL} and τ_{NL} , we consider the two-loop order corrections in the context of the iPT. In usual, these corrections can be considered as higher order effects and neglected. Of course, even in case with the pure Gaussian primordial fluctuation there exist higher order contributions which may generate the extra scale-dependency of the bias parameter. We investigated these higher order contributions in the pure Gaussian case and also in the non-Gaussian case up to the linear order in the non-linearity parameters. We find that these higher order contributions can be negligible for the range where the normalized power spectrum of the biased objects is smaller than unity, namely, $k^3 P_X(k) < 1$.

Here, we just analytically derived the bias parameter with the higher order primordial non-Gaussianity. As a future issue, hence, we have to check the validity of our formalism with performing numerical simulations and it should be interesting to consider the expected constraints for g_{NL} and τ_{NL} in the future surveys.

NOTE; During the time that we were preparing this manuscript, Ref. [24] appeared on the arXiv. In Ref. [24], the authors focused on the stochasticity due to the primordial non-Gaussianity by using the barrier crossing formalism and the peak-background split method. They derived the stochasticity coefficient which is consistent with our result in the case with Press-Schechter mass function.

Acknowledgments

This work was supported by the Grant-in-Aid for JSPS Research under Grant No. 24-2775 (SY) and also Grant-in-Aid for Scientific Research (C), 24540267, 2012 (TM).

-
- [1] T. Matsubara, Phys. Rev. D **83**, 083518 (2011) [arXiv:1102.4619 [astro-ph.CO]].
 - [2] E. Komatsu *et al.* [WMAP Collaboration], Astrophys. J. Suppl. **192**, 18 (2011) [arXiv:1001.4538 [astro-ph.CO]].
 - [3] A. Slosar, C. Hirata, U. Seljak, S. Ho and N. Padmanabhan, JCAP **0808**, 031 (2008) [arXiv:0805.3580 [astro-ph]].
 - [4] T. Matsubara, Phys. Rev. D **86**, 063518 (2012) [arXiv:1206.0562 [astro-ph.CO]].
 - [5] V. Desjacques, D. Jeong and F. Schmidt, Phys. Rev. D **84**, 061301 (2011) [arXiv:1105.3476 [astro-ph.CO]].
 - [6] A. D’Aloisio, J. Zhang, D. Jeong and P. R. Shapiro, arXiv:1206.3305 [astro-ph.CO].
 - [7] T. Suyama and M. Yamaguchi, Phys. Rev. D **77**, 023505 (2008) [arXiv:0709.2545 [astro-ph]].
 - [8] T. Suyama, T. Takahashi, M. Yamaguchi and S. Yokoyama, JCAP **1012**, 030 (2010) [arXiv:1009.1979 [astro-ph.CO]].
 - [9] N. S. Sugiyama, E. Komatsu and T. Futamase, Phys. Rev. Lett. **106**, 251301 (2011) [arXiv:1101.3636 [gr-qc]].
 - [10] V. Desjacques and U. Seljak, Phys. Rev. D **81**, 023006 (2010) [arXiv:0907.2257 [astro-ph.CO]].
 - [11] J. -O. Gong and S. Yokoyama, Mon. Not. Roy. Astron. Soc. Lett. **417**, 79 (2011) [arXiv:1106.4404 [astro-ph.CO]].
 - [12] S. Yokoyama, JCAP **1111**, 001 (2011) [arXiv:1108.5569 [astro-ph.CO]].
 - [13] D. Tseliakhovich, C. Hirata and A. Slosar, Phys. Rev. D **82**, 043531 (2010) [arXiv:1004.3302 [astro-ph.CO]].
 - [14] M. Biagetti, V. Desjacques and A. Riotto, arXiv:1208.1616 [astro-ph.CO].
 - [15] K. M. Smith and M. LoVerde, JCAP **1111**, 009 (2011) [arXiv:1010.0055 [astro-ph.CO]].
 - [16] M. LoVerde and K. M. Smith, JCAP **1108**, 003 (2011) [arXiv:1102.1439 [astro-ph.CO]].
 - [17] K. M. Smith, S. Ferraro and M. LoVerde, JCAP **1203**, 032 (2012) [arXiv:1106.0503 [astro-ph.CO]].
 - [18] T. Nishimichi, arXiv:1204.3490 [astro-ph.CO].
 - [19] T. Matsubara, Phys. Rev. D **77**, 063530 (2008) [arXiv:0711.2521 [astro-ph]].
 - [20] A. Dekel and O. Lahav, Astrophys. J. **520**, 24 (1999) [astro-ph/9806193].
 - [21] S. Matarrese, L. Verde and R. Jimenez, Astrophys. J. **541**, 10 (2000) [astro-ph/0001366].
 - [22] S. Joudaki, O. Dore, L. Ferramacho, M. Kaplinghat and M. G. Santos, Phys. Rev. Lett. **107**, 131304 (2011) [arXiv:1105.1773 [astro-ph.CO]].
 - [23] H. Tashiro and S. Ho, arXiv:1205.0563 [astro-ph.CO].
 - [24] D. Baumann, S. Ferraro, D. Green and K. M. Smith, arXiv:1209.2173 [astro-ph.CO].